

# PNM Approach to Protecting Overcompensated High-Voltage Lines

Henry Moradi, *Public Service Company of New Mexico*  
Kamal Garg, Mangapathirao V. Mynam, Eric Chua, and Jordan Bell,  
*Schweitzer Engineering Laboratories, Inc.*

**Abstract**—Public Service Company of New Mexico (PNM) initiated a project to intersect an existing 345 kV series-compensated line to feed a critical load. This system reconfiguration resulted in a series compensation of 170 percent, which is a challenge for protection engineers. This paper discusses this project, as well as the PNM protection philosophy for transmission lines. For this application, PNM applied phasor-based protection (distance, permissive overreaching transfer trip [POTT], and differential schemes) and ultra-high-speed (UHS) protection using incremental and traveling-wave-based principles. This paper also discusses challenges encountered when protecting series-compensated lines and provides a performance comparison of phasor-based and UHS protective relays. We used real-time digital simulation to evaluate the two protection systems. We also show the performance of the phasor-based and UHS-based protection schemes for an external C-phase-to-ground fault.

## I. INTRODUCTION

This paper discusses the implementation of phasor-based protection and ultra-high-speed (UHS) protection using time-domain principles on a 345 kV line in New Mexico. This line connects the east and west ends of the Public Service Company of New Mexico (PNM) utility system and is critical to the PNM system reliability.

### A. Overview of Transmission System

PNM is an investor-owned electric utility that serves its customers and provides network integration transmission services to third parties in the northern New Mexico portion of the Western Electricity Coordinating Council grid. PNM also operates 115 kV and lower voltage networks that are part of the southwestern New Mexico electric power system. PNM owns 14,338 miles of 46 kV, 69 kV, 115 kV, 230 kV, and 345 kV transmission lines. Their San Juan and Four Corners substations in northwestern New Mexico house the majority of the PNM system generation assets. Essentially, PNM designed their bulk transmission system (shown in Fig. 1) to transmit power from northwestern New Mexico to load centers in the northern half of New Mexico. Most of the PNM load is in the Albuquerque metropolitan area.

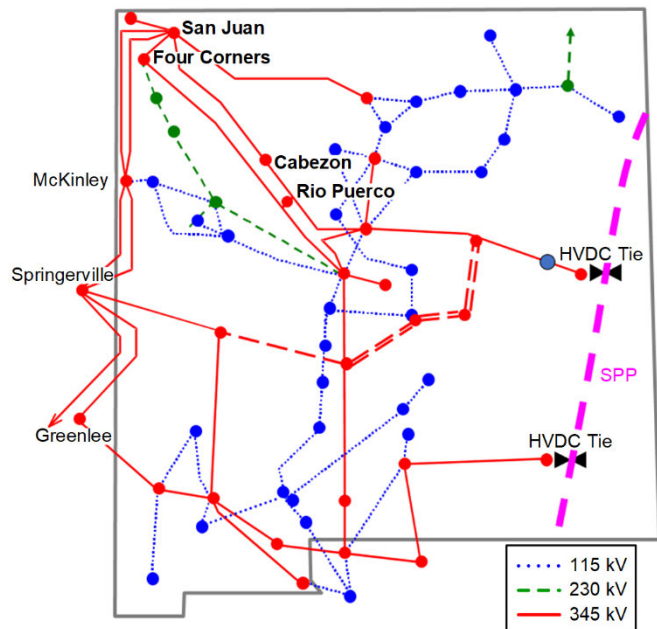


Fig. 1. PNM Transmission System Overview

### B. Cabezon Project Summary and One-Line Diagram

Fig. 2 shows the simplified one-line diagram of the 345 kV line from the PNM Cabezon substation to the Rio Puerco substation, along with the neighboring lines. The Cabezon substation is a new substation on the original San Juan–Rio Puerco line. The Cabezon substation serves critical mining loads and is part of the major east-to-west interconnection. The shunt reactor at the Rio Puerco terminal on the Cabezon–Rio Puerco line provides reactive power compensation.

Typically, PNM lines are series-compensated at one end with 50 percent compensation. The original San Juan–Rio Puerco line was 37 percent ( $-32.2 \Omega / 88 \Omega$ ) series-compensated. However, due to this system reconfiguration, the new Cabezon–Rio Puerco line is 170 percent ( $-32.2 \Omega / 19 \Omega$ ) series-compensated. Table I lists the main parameters of the Cabezon–Rio Puerco line under study in this paper.

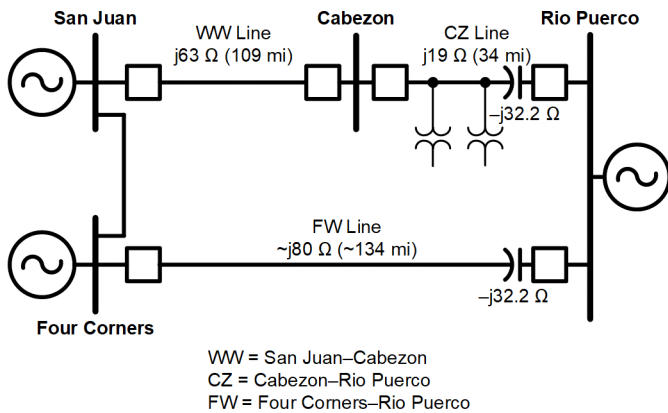


Fig. 2. 345 kV Network Including the Cabezon-Rio Puerco Line

TABLE I  
CABEZON-RIO PUERCO LINE PARAMETERS

<b>Z1</b>	2.67 Ω secondary
<b>Z0</b>	9.25 Ω secondary
<b>XC</b>	-4.285 Ω secondary
<b>Line Length</b>	34 miles

## II. PNM LINE PROTECTION STANDARDS

PNM uses both ring and breaker-and-half bus configurations in their system. The primary PNM transmission voltages are 115 kV, 230 kV, and 345 kV, with most of the transmission lines operating at 115 kV. The major PNM interconnections are at 345 kV, with a backbone system at 115 kV. The majority of the PNM lines use three-pole tripping. The existing PNM line protection standard is to use one relay at 115 kV, two relays at 230 kV, and three relays at 345 kV. The recently approved protection standard at PNM for their 345 kV lines requires that each relay be capable of line current differential and permissive overreaching transfer trip (POTT) schemes with step-distance and overcurrent protection. For the Cabezon-Rio Puerco and San Juan-Rio Puerco lines, PNM used UHS line protection based on time-domain principles.

The PNM line standard specifies four distance zones with quadrilateral characteristics for both phase and ground elements. The standard also specifies that the POTT scheme use directional ground overcurrent and overreaching distance elements [1]. The Zone 1 phase distance reach is set at 70 to 80 percent of the line impedance, and for the mutually coupled line, the Zone 1 ground reach is reduced to 50 to 80 percent based on mutual coupling. Zone 2 (phase and ground) is set to reach beyond the remote bus to provide enough reach for POTT and step-distance protection. The Zone 2 distance reach is set to 125 to 175 percent of the line impedance. Zone 3 (phase and ground) is set in the reverse direction, and the reach is selected to coordinate with the remote bus Zone 2 reach. Zone 4 (phase and ground) is set in the forward direction and acts as a remote breaker failure backup. We used system configurations to set the Zone 4 reach appropriately. However, in general, we set it to reach the longest line from the remote bus with infeed. In addition to zone protection, PNM also uses local breaker failure

protection in the majority of their substations, as well as a remote breaker failure scheme implemented in modern microprocessor-based relays on their system.

For switch onto fault (SOTF) conditions, we enabled one level of phase and ground overcurrent elements. We enabled one ground time-overcurrent element to coordinate with the remote-end relay. A delay of 0.5 seconds is desirable for the remote bus fault; however, an N-1 contingency requires a coordination time of 0.25 to 0.3 seconds.

In addition to distance protection, the PNM standard specifies differential protection. PNM has multiple tapped loads at the 115 kV voltage level that are fed from delta/wye load transformers. Hence, negative-sequence differential and negative-sequence overcurrent protection is not applied at the 115 kV voltage level. Currently, for most of these tapped loads, no breaker exists on the high side of the tapped load transformers. In the future, PNM plans to add breakers at these tapped stations. This plan will allow them to trip the high-side transformer breaker and subsequently open the high-voltage circuit switcher on the transformer (see Fig. 3). Once the circuit switcher opens, the high-side line breaker can close to restore the line. At the 230 and 345 kV voltage levels, negative-sequence differential protection is enabled.

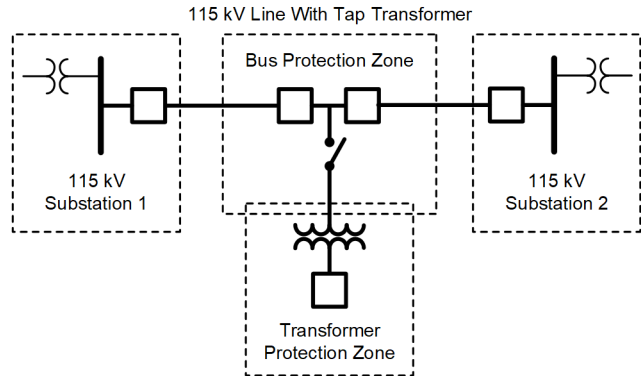


Fig. 3. Example of 115 kV Line and Tapped Transformer Protection

At the 115 kV voltage level, PNM applies single-shot reclosing. At the 345 kV voltage level, automatic reclosing is applied only on some lines based on system requirements.

The PNM philosophy is to use line relays for breaker failure protection. Fig. 4 shows their simplified breaker failure scheme for bus, line, and transformer breakers. Each breaker also has a dedicated breaker failure lockout relay. In the case of Circuit Breaker 1 (CB1) failure, the breaker failure relay first retrips the breaker. If this does not work, the relay asserts the breaker failure lockout relay after the breaker failure time. The relay sends a transfer trip to the remote end. Relay R1 also cross-trips Relays R2 and R3 to improve scheme reliability. To improve system reliability, PNM prefers to trip the breakers directly from the breaker failure relays instead of from the lockout relays. The existing practice is to use lockout relays only for blocking close commands (BCL). Fig. 4 also shows the zones of protection for bus, line, and transformer breaker failure relays. However, this paper does not discuss the details of bus and transformer protection standards.

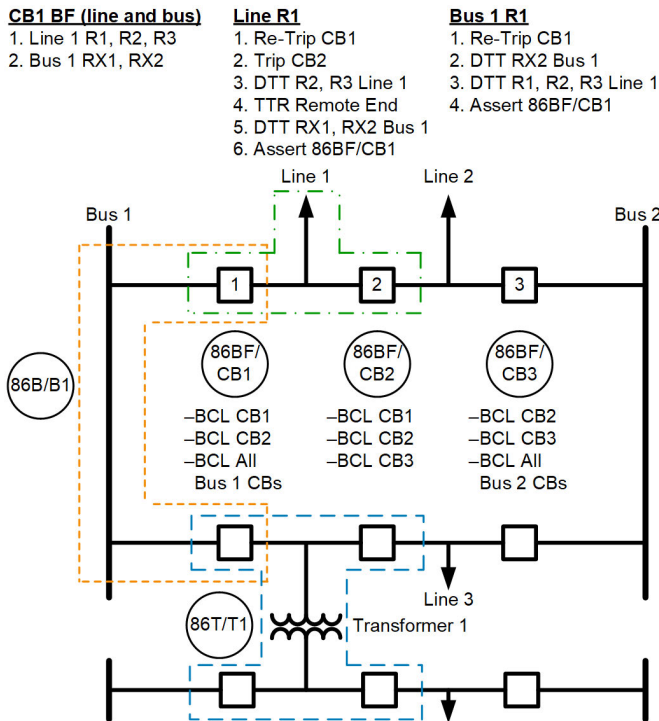


Fig. 4. Example of Breaker Failure Scheme and Zones of Protection

PNM also uses shunt reactors on 345 kV lines, which are typically installed at one end of a line. For the Cabezon–Rio Puerco line, a reactor exists at the Rio Puerco end. For line reactors, PNM uses dual-redundant differential reactor protection. Because line relays are programmed for breaker failure, reactors are also in the line differential zone. The line differential relay settings are configured to accommodate the error due to the reactor current. Fig. 5 shows the current transformer (CT) connections used for phasor and UHS relays.

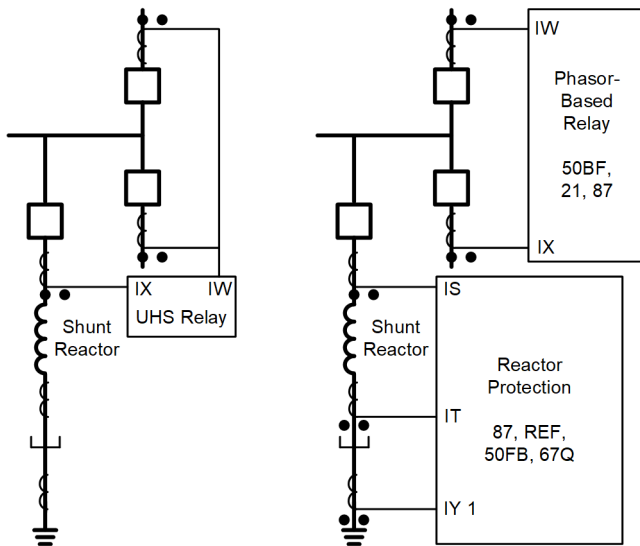


Fig. 5. Example CT Connections to the PNM Phasor and UHS Relays

PNM uses a combination of fiber-optic and digital microwave radio communications media to provide connectivity between the line protective relays deployed in all the protection schemes. The optical network consists of synchronous optical network (SONET) and wavelength-

division multiplexing equipment. Direct fiber connection between the local and remote relays is required for the traveling-wave differential [TW87] scheme. In all schemes, redundant communications circuits exist for each relay channel between the local and remote ends. PNM deploys microwave radio systems to provide subtending SONET ring configurations in some locations. PNM has three relays at extra-high voltage levels. These systems, Systems A, B, and C, use two communications channels: one on direct fiber and the other on SONET. In the case that the direct fiber channel is not available, both communications paths end up routed over SONET. For UHS relays, the TW87 scheme uses direct fiber and the POTT scheme uses SONET communications.

### III. SERIES-COMPENSATED LINES AND PROTECTION CHALLENGES

Fig. 6 shows an example of a PNM capacitor bank, with a typical capacitor rating of 1,680 A and a metal-oxide varistor (MOV) that starts to conduct at 4 kA. The bypass breaker is closed if the energy exceeds MOV limits or if the fault current is higher than a set limit.

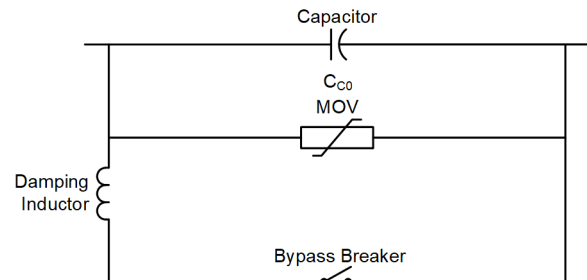


Fig. 6. PNM Typical Capacitor Bank With MOV and Bypass Breaker

Typically, engineers install series capacitors at either one or both ends of a line. This is because space is often available inside a substation for these capacitors, which helps keep installation costs down. However, it is also possible to install series capacitors on a line in a central location [2]. On the Cabezon–Rio Puerco line, the series capacitor is at the Rio Puerco terminal.

During faults, series capacitors are exposed to large transient fault currents and, as a result, to large voltages. If the series capacitor is not protected, this large voltage exposure can cause significant damage. To address this, MOVs are often installed in parallel with series capacitors to help prevent capacitor damage. An MOV works by clamping the voltage magnitude across the capacitor to within the capacitor operational limits. During a fault, the voltage across the capacitor increases and then exceeds the MOV reference voltage. In response, the MOV starts conducting and operates like a variable resistor.

The following subsections discuss some of the known challenges of series-compensated lines.

#### A. Voltage and Current Inversion Challenges

For a fault near a capacitor on a series-compensated line, a voltage inversion can take place if the impedance from the relay to the fault is capacitive (not inductive). Additionally, a voltage inversion may affect directional and distance elements within a

relay. However, modern line relay internal logic can detect voltage inversion conditions and use memory polarization to provide security for mho elements. Moreover, directional elements can generally correctly determine the direction of a fault as long as there is no current inversion condition on the line as well [3].

A current inversion can affect both directional and differential discrimination. For an internal fault on a series-compensated line, a current inversion takes place when the equivalent system is capacitive on one side of the fault and the system on the opposite side is inductive. In this situation, current outfeed occurs, which is when the current flows out of a line at one terminal.

Spark gaps or MOVs installed to help protect series-compensated lines bypass the series capacitor for most bolted, high-current faults. On the other hand, the low fault current levels for high-resistance and single-phase-to-ground faults prevent the bypass and create current inversion conditions. Current inversion can affect elements that operate using phase-component or sequence-component quantities, including distance, differential, directional, and phase-comparison elements.

### B. Series Capacitors and Line Impedance Estimation Challenges

Because of the interactions of series capacitors with the lines they are installed on, a capacitor can introduce errors to the estimated line impedance measured by impedance-based protective elements in a relay. In addition, the estimated impedance can oscillate as a result of subharmonic frequency oscillations [4]. Therefore, the impedance estimate on series-compensated lines depends on the state of the capacitor protection (MOV and bypass breaker). Fault analysis using short-circuit programs can determine the apparent impedance seen by the relays.

Fig. 7 shows the capacitor bank impedance of the Cabezon–Rio Puerco line in per unit (pu) and the MOV protection level. The following are the capacitor bank impedance calculations for this project:

- Series capacitor (X) =  $-0.027$  pu
- $Z_{base} = kV^2 / MVA = 3,452 / 100 = 1,190 \Omega$
- $Z_{cap\_PRI} = X_c \cdot Z_{base} = -32.14 \Omega$
- $Z_{cap\_SEC} = Z_{cap\_PRI} \cdot CTR / PTR = -32.14 \cdot 400 / 3,000 = -4.285 \Omega$

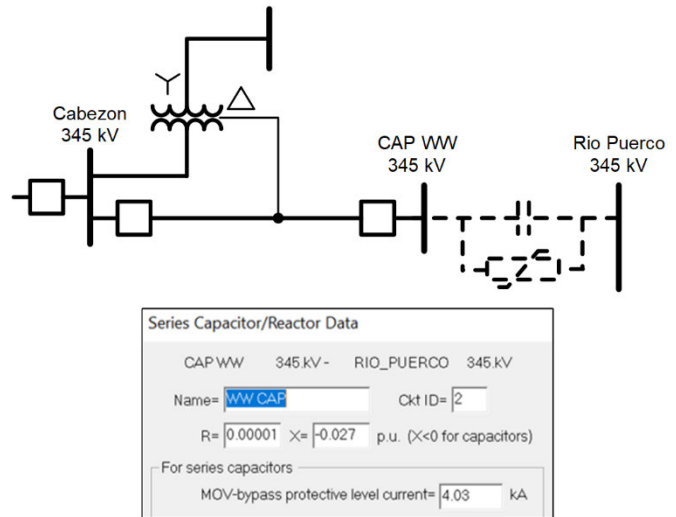


Fig. 7. Capacitor Bank Size and MOV Protection Level

Fig. 8 shows the apparent impedance seen by the relays on the PNM system. In this case, the fault current is lower than the capacitor MOV rating. Hence, the MOVs did not bypass the capacitors and the actual line impedance seen by the relays is negative.

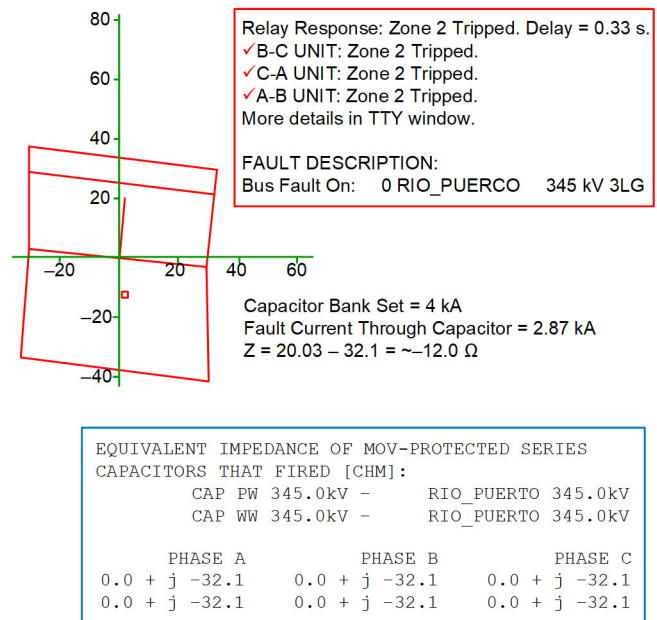


Fig. 8. Measured Impedance and State of MOV

In another example of two capacitor banks, the MOV for one capacitor does not bypass the capacitor (the fault current is lower than the MOV rating). However, another capacitor bank MOV starts conducting and the capacitor appears as a parallel combination of resistor and capacitor. Hence, lines with series capacitor banks need to be analyzed for various operating conditions and fault levels to make sure that the zone reach selections are adequate for various faults and operating conditions [5].

Fig. 9 shows an example of the San Juan–Rio Puerco and Four Corners–Rio Puerco line capacitor banks at Rio Puerco. For a three-phase fault at the Cabezon substation bus, the capacitor bank MOV on the Four Corners–Rio Puerco line at the Rio Puerco end starts conducting.

1. Bus Fault on:					
0 Cabezon		345. kV 3LG			
BUS	0 Cabezon	345.KV	AREA	1	ZONE
			+ SEQ		
VOLTAGE (KV. L-G)			> 0.000@ 0.0		
BRANCH CURRENT (A) TO			>		
63	SAN JUAN	345.	1L	2456.2@	99.3
0	CAP WW	345.	1L	6858.4@	131.3
0	Terreon-TRIS	115.	1X	71.2@	110.5
0	13.8 Cabezon	13.8	1X		

PHASE A		PHASE B		PHASE C	
0.0 + j	-32.1	0.0 + j	-32.1	0.0 + j	-32.1
10.8 + j	-18.5	10.8 + j	-18.5	10.8 + j	-18.5

Fig. 9. MOV and Capacitor Bank Equivalent Impedances (Four Corners–Rio Puerco and San Juan–Rio Puerco Lines at Rio Puerco End)

### C. Differential Protection Challenges

For this project, the line differential scheme was based on percentage differential elements. These elements function by comparing the operating current signal with the restraining current signal. If the operating current is greater than a percentage of the restraining current and greater than a set minimum pickup current threshold, the differential element operates.

Fig. 10 shows that for external faults, load flow situations, or other ideal through-current conditions, the magnitudes of the local current,  $\bar{I}_L$ , and the remote current,  $\bar{I}_R$ , are equal, and the currents are out of phase (180 degrees apart). In contrast, for internal faults under ideal conditions, both of these currents are in phase.

Sometimes during internal faults, current may flow out of a line at one terminal. For a series-compensated line application, this outfeed takes place when one source reactance to the fault is capacitive. If the internal fault is a high-resistance fault, this condition can also cause current outfeed. Modern differential relays are capable of detecting internal faults correctly for outfeed conditions.

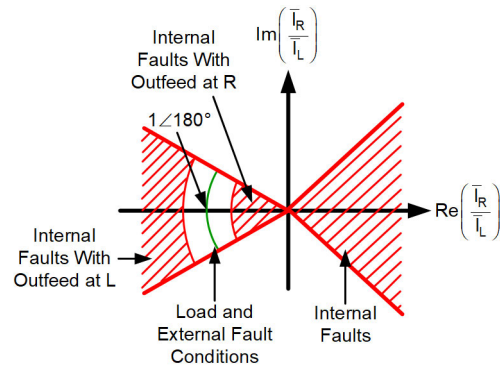


Fig. 10. Example Differential Protection Operating Condition for Power System Load and Fault Conditions [2]

## IV. PNM PROTECTION PHILOSOPHY AND SELECTED PROTECTION SCHEME FOR CABEZON–RIO PUERCO LINE

This section discusses the various protection elements in the phasor-based and UHS relays selected to protect this critical Cabezon–Rio Puerco line.

### A. Solution Using Existing Phasor-Based Protection Principles

#### 1) Distance Reach Selection

The potential transformers are on the line side at both the Cabezon and Rio Puerco terminals (see Fig. 2). At the Cabezon end, the net line impedance is negative, and it is not possible to set Zone 1. At the Rio Puerco end, we set Zone 1 to 70 percent of the line impedance for both phase and ground quadrilateral elements. Based on previous experience, PNM uses a resistive reach of 30  $\Omega$  primary for Zone 1.

We set the Zone 2 reach at 125 percent of the line impedance at both ends. We used Zone 2 in both POTT and step-distance schemes and configured a step-distance time delay of 20 cycles. We set the Zone 3 reverse reach at 125 to 150 percent of the remote Zone 2 forward reach. We selected the Zone 4 forward reach for breaker failure, with the goal to cover the longest line from the remote terminal with infeed and with a time delay of 60 cycles. We selected one level of the high-set instantaneous directional overcurrent (phase and ground) element to provide protection for 10 to 20 percent of the line. Additionally, we enabled one directional ground time-overcurrent backup element with a time delay of 30 cycles to clear a remote bus ground fault. This element is coordinated with ground overcurrent elements on other lines.

#### 2) Line Current Differential Settings

The line standard specifies a CT ratio of 2000:5 for high-voltage lines. We enabled positive-, negative-, and zero-sequence differential elements for this application. The positive-sequence differential element sensitivity is set above

line charging and maximum load unbalance current. A line reactor exists at the Rio Puerco end, and we considered the reactor current in selecting the phase differential pickup. Reactor current is not subtracted from the total current in the line relays. For positive-sequence current, we used settings of 600 A primary, or  $600 \text{ A} / 2,000 \text{ A} = 0.3 \text{ pu}$ . We used alpha plane settings of 6.0 radius and 95 degrees for this application. Laboratory tests validated these settings. The ground differential element sensitivity was selected at 200 A, considering a 10 to 15 percent maximum unbalance, or  $200 \text{ A} / 2,000 \text{ A} = 0.1 \text{ pu}$ . We also enabled the negative-sequence differential element since there is no tapped load, and laboratory tests proved the setting of 500 A (or 0.25 pu) to be secure and sensitive.

### B. UHS Relay Configuration

UHS time-domain relays use incremental quantities and traveling waves to provide operating times on the order of a few milliseconds. Reference [6] discusses the following UHS protection principles:

1. A Zone 1 underreaching distance element using incremental quantities.
2. A POTT scheme using an incremental quantity directional element (TD32) and a traveling-wave directional element (TW32).
3. A TW87 scheme using current traveling waves.

It is challenging to configure line protection on series-compensated lines. As discussed in Section III, configuring line protection in these applications requires detailed transient simulations and analysis. During a fault, series capacitors tend to appear as short circuits at first. Because of this, time-domain relays that operate on transient components of faults usually perform better when they are applied in series-compensated line schemes.

### C. Configuring UHS Time-Domain Line Protection on Cabezon–Rio Puerco Line

This section documents the procedure to configure the time-domain protection functions on the PNM Cabezon–Rio Puerco line. At the Rio Puerco terminal, an in-zone shunt reactor is available for shunt compensation. To accommodate the line reactor and the breaker-and-a-half scheme, the reactor CT is connected to Relay Terminal X and the two paralleled breaker CTs are connected to Relay Terminal W. Providing the reactor current allows the relay to measure the effective line current, making it remain secure during reactor switching operations. Fig. 5 shows the CT configuration at the Rio Puerco terminal. To detect an open pole at this terminal, the relay uses currents measured on Relay Terminal W.

#### 1) Distance Element (Incremental Quantity)

We set the Zone 1 phase and ground distance elements to 75 percent and 70 percent of the line, respectively, at both terminals. Because the TD21 element restraining signals account for the in-line series capacitance, we configured the reach settings based on the line impedance and not on the net impedance of the line and series capacitor. The total capacitor

reactance setting was set equal to the in-line series capacitance value at the Cabezon terminal, and the external series compensation setting at the Cabezon terminal was set to Y to account for the series capacitor behind the Rio Puerco terminal on the Four Corners–Rio Puerco line. With the capacitively coupled voltage transformer on the line side at the Rio Puerco terminal, we set the total capacitor reactance setting to 0. In line with the recommendation detailed in [7], we configured the external series compensation setting to Y to provide security for the TW87 scheme.

#### 2) POTT Scheme

We configured the POTT scheme to use an incremental quantity-based directional element. The incremental quantity-based directional element uses forward and reverse impedance threshold settings to declare the direction of the event. We set the forward impedance threshold, TD32ZF, to 30 percent of the positive-sequence system impedance (the strongest source) behind the relay. We used a short-circuit program to calculate the strongest source impedances behind the Cabezon and Rio Puerco terminals. Based on these values, we set TD32ZF to  $16.25 \text{ } \Omega$  primary and  $8.7 \text{ } \Omega$  primary at the Cabezon and Rio Puerco terminals, respectively. We set the reverse impedance threshold, TD32ZR, to 30 percent of the sum of the positive-sequence impedance of the line (including the series capacitor, if it is in-zone) and the remote positive-sequence source impedance (the strongest source). We set TD32ZR to  $1.23 \text{ } \Omega$  primary and  $1.04 \text{ } \Omega$  primary at the Cabezon and Rio Puerco terminals, respectively.

Since the line is series-compensated, we set the POTT overcurrent supervision levels (TP67P and TP67G) to greater than the maximum incremental current caused by switching of the line series capacitor bank. Equation (1) was used to calculate the maximum incremental current resulting from capacitor switching. This calculation uses the strongest equivalent source impedance for the local source and the remote source.

$$TP67G = \frac{1.25}{\sqrt{3}} \cdot \frac{VNOM}{|Z_{S1} + Z_{L1} + Z_{T1}|} \quad (1)$$

where:

$Z_{S1}$  is the strongest local source impedance.

$Z_{L1}$  is the line impedance.

$Z_{T1}$  is the strongest equivalent remote source impedance.

We set the POTT overcurrent supervision levels, TP67P and TP67G, to 3.47 A and 6.48 A, respectively. The relay uses an effective dynamic threshold based on the user-provided overcurrent supervision threshold and measured voltage drop across the series capacitor. This approach provides POTT scheme dependability without compromising security during series capacitor switching. Two redundant communications channels exchange the POTT signals; one channel is point-to-point direct fiber and the other is an IEEE C37.94-based multiplexed channel. In addition to the POTT signals, these communications channels exchanged direct transfer trip signals.

### 3) TW87 Scheme

A TW87 scheme uses current traveling waves. Measuring traveling-wave line propagation time (TWLPT) is the first step to configuring a TW87 scheme. During commissioning, the Rio Puerco terminal was closed and the Cabezon terminal was open. We configured the relay to trigger event recording during the line pickup. Fig. 11 shows the captured phase currents and voltages sampled at 1 MHz. The phase currents show that Pole C closed first, followed by Pole B and Pole A.

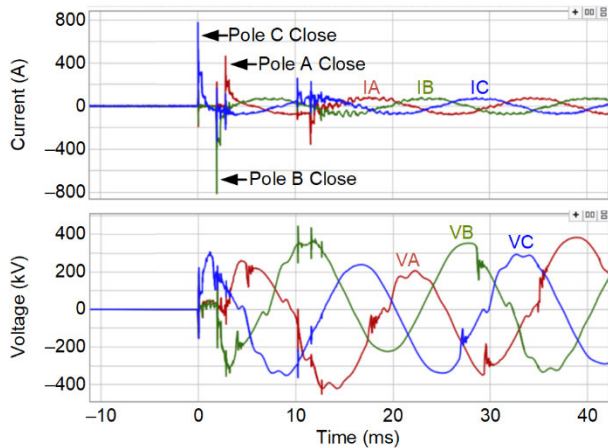


Fig. 11. Phase Currents and Voltages Captured at the Rio Puerco Terminal During Line Energization

Fig. 12 shows the high-frequency signal associated with the A-phase current (the last pole closed) used to measure the round-trip time of the Cabezon–Rio Puerco line. We set the TWLPT setting in the relay to  $186.87 \mu\text{s}$ .

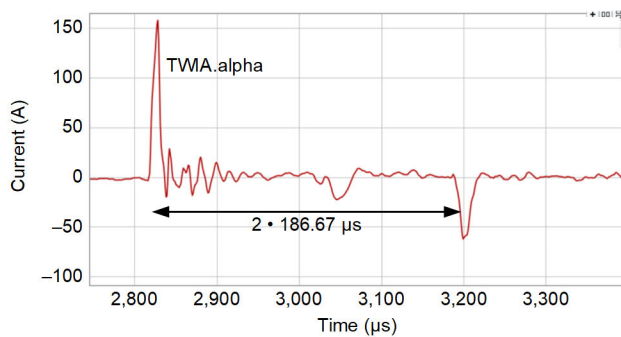


Fig. 12. High-Frequency Signal for A-Phase Current; TWLPT Is Configured to  $186.87 \mu\text{s}$

The TW87 scheme has supervisory overcurrent elements that provide security for events such as lightning strikes and switching events. Series capacitor switching launches waves of opposite polarities, which is a pattern for an external event. Therefore, in-line series capacitor switching does not jeopardize the security of the TW87 scheme.

## V. LABORATORY TESTS AND FIELD EVENT RESULTS

Due to the challenges discussed in Section III, many utilities consider performing hardware-in-the-loop testing to validate line protection schemes when applying them on series-compensated lines. This section provides details about the extensive laboratory testing performed to validate the settings and design for this critical PNM project.

### A. Real-Time Digital Simulation

To validate the protection system, a real-time digital simulator was used to perform closed-loop testing. The overall system short-circuit model was reduced to an equivalent network that was modeled in the transient environment. This equivalent network was composed of 11 substations, including the bulk of the PNM 345 kV transmission system, with equivalents at the 345 kV voltage level and in the neighboring utilities.

PNM system planning and protection engineers collaborated to determine the following realistic system operating conditions that would test the protection system:

- System normal.
- System weak behind each terminal.
- Parallel transmission paths out of service.

### B. Test System One-Line Diagram

Fig. 13 shows the one-line diagram of the real-time digital simulation system model. This model simulated faults on the line under study (Cabezon–Rio Puerco) and on the neighboring lines to test the protection system.

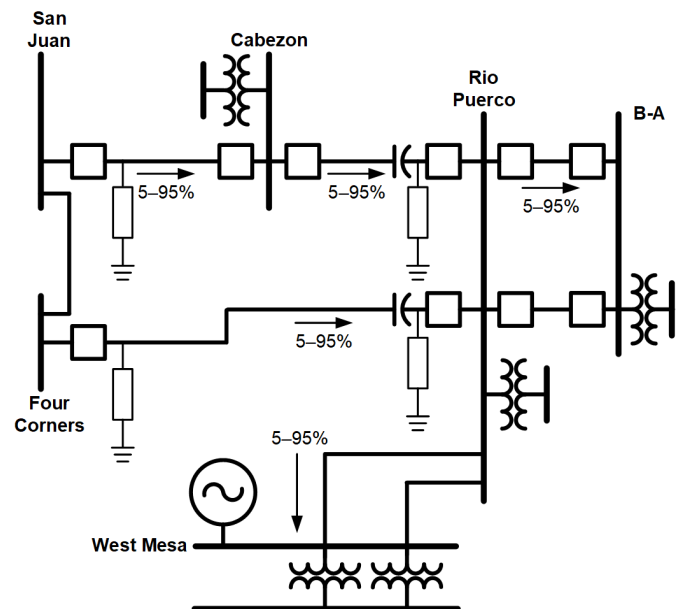


Fig. 13. Simulated Network to Test the Performance of the Protective Relays

### C. Test Procedure

We tested all three relays protecting the Cabezon–Rio Puerco line simultaneously and analyzed the results to confirm proper operation. Table II lists the tests used to verify the performance of the protective relays on the Cabezon–Rio Puerco line. References [8], [9], [10], and [11] discuss typical hardware-in-the-loop tests used to verify the performance of line protection.

TABLE II  
TEST PLAN

Test Number	Test Procedure
1	Internal and external faults
2	Line energization and load pickup
3	Zone 1 margin
4	High-impedance faults
5	SOTF
6	Evolving faults
7	Cross-country faults
8	Bolted fault batch tests
9	Internal high-impedance fault batch tests

We validated the settings and system setup by analyzing the results from Tests 1 through 7. We ran batch tests once the performance of the protective relays for these tests was satisfactory. A typical batch test consists of the following:

- All power flow cases.
- All internal and external fault locations (~20 locations).
- Ten fault types (AG, BG, CG, ABG, BCG, CAG, AB, BC, CA, and ABCG).
- Four points on wave (0, 30, 60, and 90 degrees).

Running the batch tests resulted in more than 6,000 individual faults applied to the protection system. The real-time digital simulator saves oscillography records for each fault and stores them in IEEE Common Format for Transient Data Exchange (COMTRADE) files. The real-time digital simulator also saves space-delimited text files that contain the elapsed time between fault initiation and element assertion for relevant digital signals obtained from the output contacts of the relays.

We analyzed the test results using readily available software and custom macros for the multiple faults. This analysis revealed the average and maximum trip times of the relays for faults along the line as well as the coverage of the Zone 1 and overcurrent elements for these faults.

We then investigated the batch test results for undesired operations and poor scheme performance. When encountering undesired operations, the project team analyzed event records

and modified the settings. After discovering root cause, the project team also proposed and validated the necessary modifications to improve the relay performance.

### D. Simulation Test Results

This section covers some of the test results and the overall performance of the protection system.

#### 1) Distance Element Performance

As discussed previously, we disabled the Zone 1 phasor-based distance element at the Cabezon terminal. Fig. 14 and Fig. 15 show the dependability results of the phasor-based and incremental quantity-based Zone 1 distance elements, respectively.

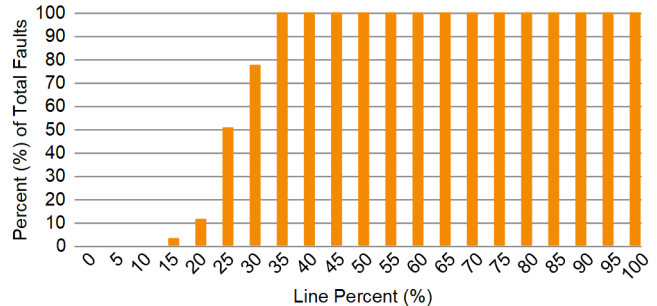


Fig. 14. Phasor-Based Zone 1 Dependability for Faults Along the Line at the Rio Puerco Terminal

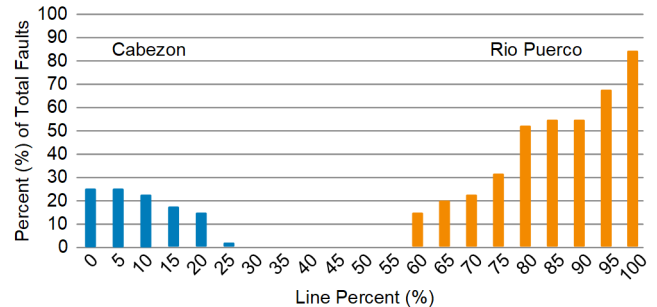


Fig. 15. Time-Domain Zone 1 Dependability for Faults Along the Cabezon–Rio Puerco Line

The TD21 time-domain distance element dependability is restricted on series-compensated line applications; the design of this element is biased toward security. The TD21 element is secure for out-of-zone faults. The POTT scheme in the UHS relay provided 100 percent dependability with security.

#### 2) Average and Maximum Trip Times

Fig. 16 shows the comparison of phasor-based and UHS-based relays. These results were obtained with the communications schemes enabled. The UHS-based relays operated in 2 to 4 ms, and the operation time of the phasor-based relays was close to 1 cycle. During this testing, for the UHS relays, we tested only incremental quantity-based protection elements and schemes.

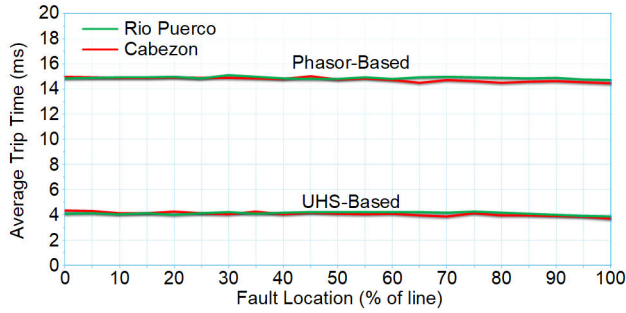


Fig. 16. Cabezon–Rio Puerco Line Operating Times of Phasor and UHS Relays

### E. Field Results

This section analyzes relay performance using field events. PNM reported more than 8 external events following the installation of phasor-based and UHS protection systems. Table III shows three of these external events for which the protection system captured event records. This section discusses the C-phase-to-ground event on August 13, 2018 in detail to show the performance of the two protection systems.

TABLE III  
EXTERNAL FAULT LOCATIONS AND DATE

Fault Date	Fault Type	Location
10/2/2018	C-phase-to-ground	Behind San Juan terminal
10/3/2018	C-phase-to-ground	Behind San Juan terminal
8/13/2018	C-phase-to-ground	Four Corners–Rio Puerco line

#### 1) UHS Protective Relay

##### a) Cabezon Terminal

Fig. 17 shows the phase currents and voltages captured at the Cabezon terminal of the Cabezon–Rio Puerco line for a C-phase-to-ground fault on the Four Corners–Rio Puerco line. The fault was 9 miles from the Rio Puerco terminal.

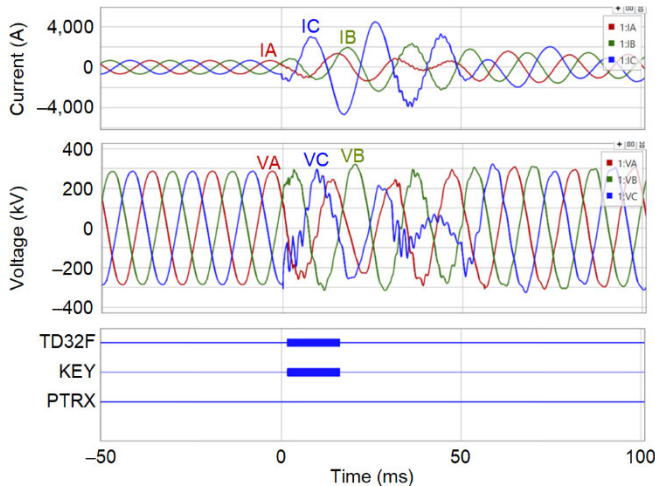


Fig. 17. Incremental Quantity and Phasor-Based Directional Elements at Cabezon Declared the Event as Forward

Fig. 18 shows the incremental loop voltage and replica current for this fault. For a forward event, these signals are

opposite in sign, and the ratio of their magnitudes is equal to the source impedance magnitude.

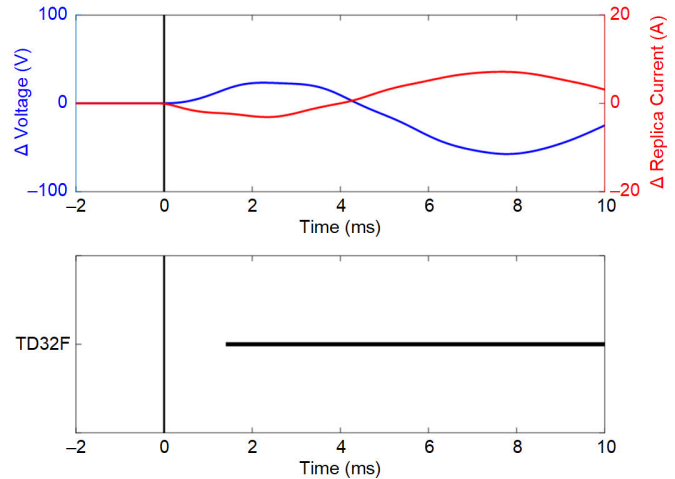


Fig. 18. Incremental Voltage and Loop Replica Current Are Opposite in Polarity for This Forward Event

The source impedance behind the Cabezon terminal can be calculated based on the ratio of the incremental voltage to the incremental replica current, and the source impedance was equal to  $7.6 \Omega$  secondary.

Fig. 19 shows the operating torque, forward restraining torque, and reverse restraining torque. For this forward event, the operating torque exceeded the forward restraining torque, asserting the TD32F element. As expected, the Rio Puerco terminal did not send the permissive key signal; therefore, the POTT scheme restrained from operating.

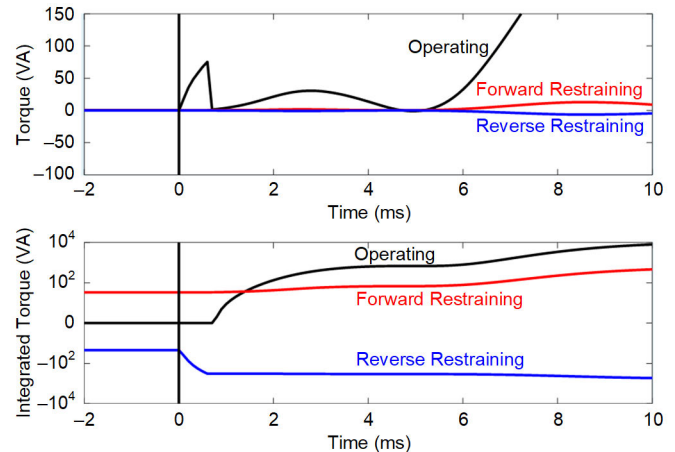


Fig. 19. C-Phase Integrated Operating Torque Exceeds the Integrated Forward Restraining Torque for the Forward C-Phase-to-Ground Fault

Fig. 20 shows the operating and restraining quantities associated with the TD21 element. For this fault beyond Zone 1, the operating quantity was less than the restraining quantity. When the external series compensation is set to Y, the TD21 element uses a more conservative restraint (static restraint) to offer security in systems with series compensation.

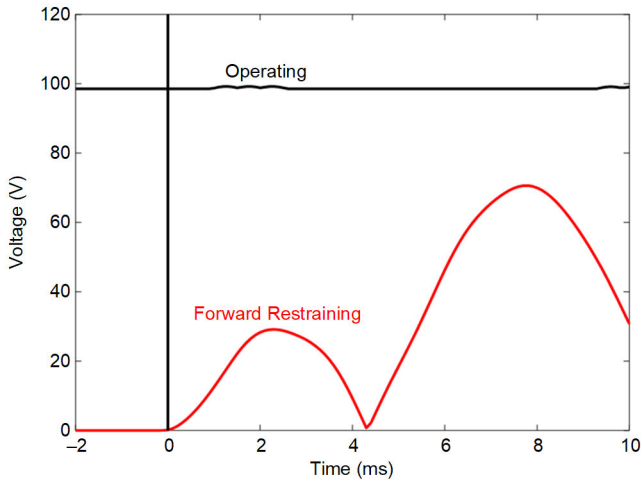


Fig. 20. C-Phase Operating Quantity Is Less Than the Restraint Quantity for This Out-of-Zone Fault

*b) Rio Puerco Terminal*

The fault was 9 miles from the Rio Puerco terminal, and the incremental quantity-based directional element asserted reverse for this event. Fig. 21 shows the phase currents and voltages recorded at the Rio Puerco terminal for this reverse event. As expected, this terminal received the permissive key signal from the remote terminal, but locally, the TD32 declared reverse, which restrained the POTT scheme.

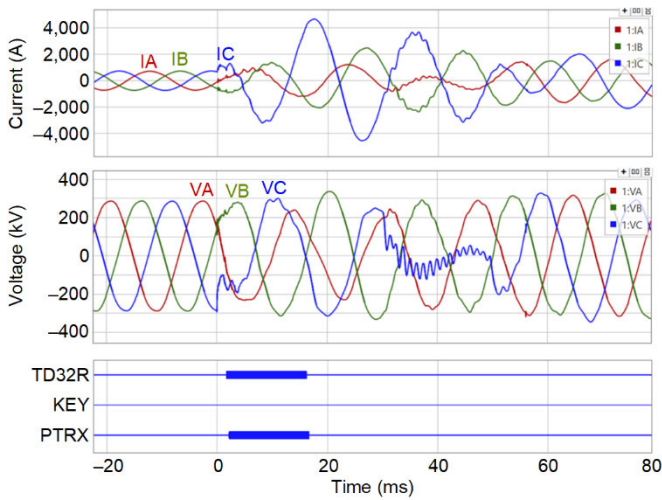


Fig. 21. TD32 Declared Reverse Event for This C-Phase-to-Ground Fault Behind the Terminal

Fig. 22 shows the incremental quantity C-phase voltage and C-phase loop replica current for this external event. The signals have the same polarity. The TD32R element asserted within 2 ms.

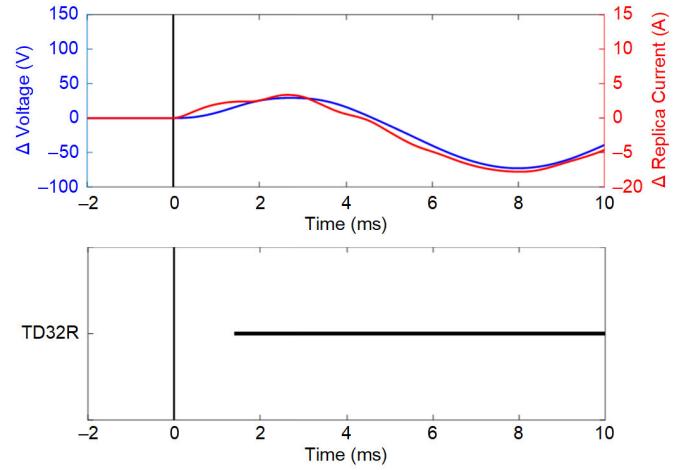


Fig. 22. Incremental Voltage and Loop Replica Current Are of the Same Polarity

The integrated operating torque is less than the integrated reverse restraining torque for this event. Fig. 23 shows the torques and the associated integrated torques.

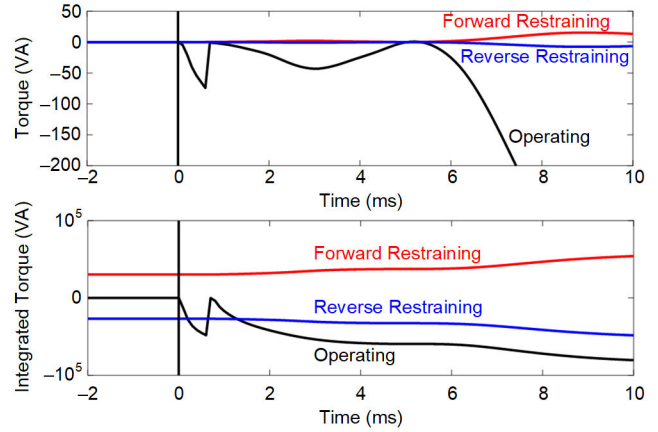


Fig. 23. Integrated Operated Torque Is Less Than the Integrated Reverse Restraining Torque

Fig. 24 shows the traveling waves (alpha mode currents associated with the C-phase reference) captured at the Rio Puerco and Cabezon terminals. Because the fault is behind the Rio Puerco terminal, the wave entered the Rio Puerco terminal. After the TWLPT (186.67  $\mu$ s), the wave exited the Cabezon terminal with opposite polarity. The TW87 scheme restrained for this external event. It is interesting to note that the reflections from the fault were recorded at both terminals. The timing difference between the first wave and the reflection from the fault (100.84  $\mu$ s) allows the fault location to be estimated at 8.94 miles from Rio Puerco.

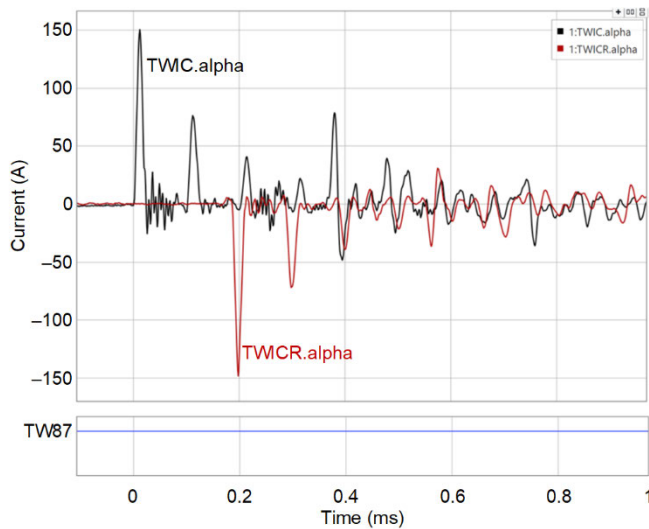


Fig. 24. The TW87 Scheme Restrained for This External C-Phase-to-Ground Fault

The PNM system around the Cabezon–Rio Puerco line has experienced many external events, and the UHS relays have remained secure for all of them. The directional elements operated within 2 ms for each one.

2) Phasor-Based Protection System

The phasor-based relays at both terminals also operated correctly for all the reported external faults on the PNM system. Fig. 25 shows the relay performance on the Cabezon–Rio Puerco line at the Cabezon terminal for the C-phase-to-ground fault on August 13, 2018. As previously mentioned, the Zone 1 underreaching element is disabled at this terminal. The Zone 2 element and directional ground overcurrent element, which are part of the POTT scheme, asserted the KEY signal.

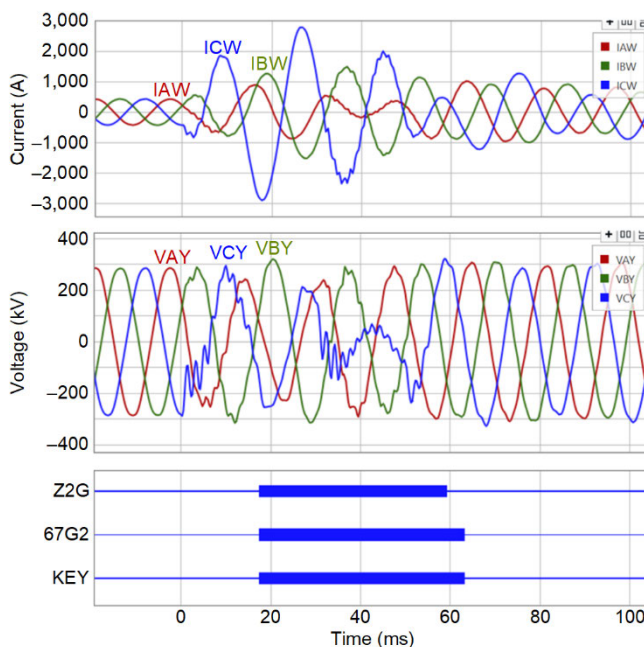


Fig. 25. Forward Elements Asserted, Declaring a C-Phase-to-Ground Fault at the Cabezon End

Fig. 26 shows the directional overcurrent and the Zone 3 reverse element performance at the Rio Puerco terminal for this fault. The POTT and differential scheme restrained from operating for this external fault.

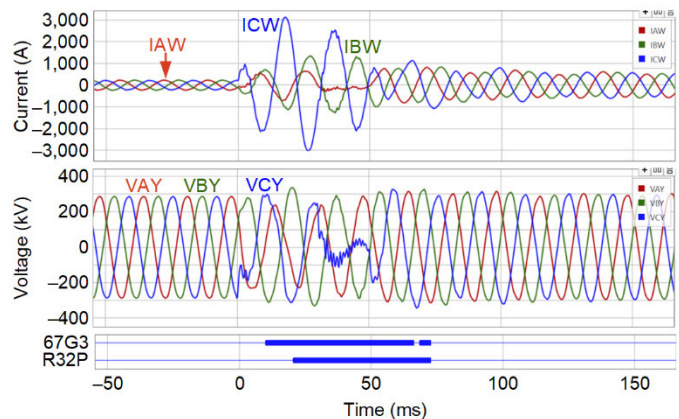


Fig. 26. Reverse Elements Asserted, Declaring a C-Phase-to-Ground Fault at the Rio Puerco End

VI. CONCLUSION

PNM segmented their existing series-compensated San Juan–Rio Puerco line to connect to their new Cabezon terminal. This segmentation resulted in 170 percent compensation on the new Cabezon–Rio Puerco line. PNM initiated a project to install UHS time-domain line protection and phasor-based protective relays to protect this 345 kV series-compensated line, and these relays are currently in service. UHS relays using incremental quantities and traveling waves respond to events prior to the voltage change across the capacitor bank; hence, these relays are better-suited for series-compensated lines than traditional relays. This paper discusses this new installation and summarizes the protection challenges for series-compensated lines.

The paper presents the PNM line protection standard and how the time-domain line protection scheme and phasor-based line protective relays were applied on the Cabezon–Rio Puerco line. The PNM project team verified the results from extensive hardware-in-the-loop simulations and are satisfied with the performance of these two protective relays. During laboratory tests, the UHS relays operated in 2 to 4 ms, and the operating time of the phasor-based relays was close to 16 ms.

Several external faults occurred on the PNM system after this project was completed that tested the security of the UHS and phasor-based protective relays. This paper shows the analysis of one C-phase-to-ground external event behind the Rio Puerco terminal. It presents the operating and restraining signals associated with the TD32 and TD21 elements and the TW87 scheme to demonstrate the UHS relay performance. Both relays restrained for this fault and all the other external events on the system.

## VII. REFERENCES

- [1] F. Calero, A. Guzmán, and G. Benmouyal, "Adaptive Phase and Ground Quadrilateral Distance Elements," proceedings of the 36th Annual Western Protective Relay Conference, Spokane, WA, October 2009.
- [2] H. J. Altuve, J. B. Mooney, and G. E. Alexander, "Advances in Series-Compensated Line Protection," proceedings of the 62th Annual Conference for Protective Relay Engineers, College Station, TX, March 2009.
- [3] J. B. Mooney and G. E. Alexander, "Applying the SEL-321 Relays on Series-Compensated Systems," SEL Application Guide (AG2000-11), 2000. Available: selinc.com.
- [4] A. Guzmán, J. Mooney, G. Benmouyal, N. Fischer, and B. Kasztenny, "Transmission Line Protection System for Increasing Power System Requirements," proceedings of the International Symposium Modern Electric Power Systems (MEPS), Wroclaw, Poland, September 2010.
- [5] E. Bakie, C. Westhoff, N. Fischer, and J. Bell, "Voltage and Current Inversion Challenges When Protecting Series-Compensated Lines – A Case Study," proceedings of the 69th Annual Conference for Protective Relay Engineers, College Station, TX, April 2016.
- [6] E. O. Schweitzer, III, B. Kasztenny, A. Guzmán, V. Skendzic, and M. V. Mynam, "Speed of Line Protection – Can We Break Free of Phasor Limitations?," proceedings of the 68th Annual Conference for Protective Relay Engineers, College Station, TX, March 2015.
- [7] B. Kasztenny, "Distance Protection of Series Compensated Lines – Problems and Solutions," proceedings of the 28th Annual Western Protective Relay Conference, Spokane, WA, October 2001.
- [8] D. Erwin, M. Anderson, R. Pineda, D. A. Tziouvaras, and R. Turner, "PG&E 500 kV Series-Compensated Transmission Line Relay Replacement: Design Requirements and RTDS® Testing," proceedings of the 64th Annual Conference for Protective Relay Engineers, College Station, TX, April 2011.
- [9] F. Plumptre, M. Nagpal, X. Chen, and M. Thompson, "Protection of EHV Transmission Lines With Series Compensation: BC Hydro's Lessons Learned," proceedings of the 62nd Annual Conference for Protective Relay Engineers, College Station, TX, March 2009.
- [10] G. Corpuz, K. Koellner, J. Bell, S. Rajan, A. Somani, and M. Thompson, "Series-Compensated Line Protection Challenges in the CREZ Region," proceedings of the 67th Annual Conference for Protective Relay Engineers, College Station, TX, March 2014.
- [11] D. Bucco, C. Sanden, A. Torres, E. Wong, J. Bell, N. Fischer, and J. Thompson, "Protection Challenges for North America's First Combined Cable/Overhead Double-Circuit 500 kV Transmission Line With Mutual Coupling," proceedings of the 70th Annual Conference for Protective Relay Engineers, College Station, TX, April 2017.

## VIII. BIOGRAPHIES

**Henry Moradi** is the Manager of the Transmission Engineering Department for Public Service Company of New Mexico (PNM). In this position, Henry manages Protection & Controls, Substation Designs, Transmission Lines, and Telecommunication Engineering groups. Prior to joining PNM, he held various engineering positions at NV Energy in Las Vegas, Nevada, performing power system and protection studies, substation designs, and controls and automation engineering. He received BS degrees in electrical engineering from the University of Nevada, Las Vegas. He is a registered professional engineer in New Mexico and Nevada.

**Kamal Garg** received his MSEE from Florida International University and India Institute of Technology, Roorkee, India, and his BSEE from Kamla Nehru Institute of Technology, Avadh University, India. Kamal worked for POWERGRID India and Black & Veatch for several years at various positions before joining Schweitzer Engineering Laboratories, Inc. (SEL) in 2006. Presently, he is a senior protection engineer at SEL Engineering Services, Inc. (SEL ES). Kamal has experience in protection system design, system planning, substation design, operation, remedial action schemes, synchrophasors, testing, and maintenance. Kamal is a licensed professional engineer in the U.S. and Canada and a senior member of IEEE and member of many working groups in IEEE PSRC.

**Mangathirao (Venkat) Mynam** received his MSEE from the University of Idaho in 2003 and his BE in electrical and electronics engineering from Andhra University College of Engineering, India, in 2000. He joined Schweitzer Engineering Laboratories, Inc. (SEL) in 2003 as an associate protection engineer in the SEL Engineering Services, Inc. (SEL ES) division. He is presently working as a principal research engineer in SEL research and development. He was selected to participate in the U. S. National Academy of Engineering (NAE) 15th Annual U. S. Frontiers of Engineering Symposium. He is a senior member of IEEE and holds patents in the areas of power system protection, control, and fault location.

**Eric Chua** received his MSc in power systems from the University of Bath, U.K., in 2004, and he earned an MBA and BEng (Hons) from the University of Malaya, Malaysia, in 1999 and 1992, respectively. Eric started his career as a protection and control design engineer, and then he worked as an application engineer and a technical manager at GEC/ALSTOM Malaysia before moving to the U.S. in 1999. Prior to joining Schweitzer Engineering Laboratories, Inc. (SEL) in 2012, Eric was a senior consulting electrical engineer in the water and wastewater industry. Presently, he is a senior protection engineer at SEL Engineering Services, Inc. (SEL ES). He has experience in protection system design, system planning, substation design, operation, event report analysis, electrical system studies, relay settings, testing, and commissioning. Eric is a licensed professional engineer in California, Nevada, Arizona, and Michigan, and he is a member of IEEE.

**Jordan Bell** received his BSEE from Washington State University in 2006. He joined Schweitzer Engineering Laboratories, Inc. (SEL) in 2008 as a protection engineer in the SEL Engineering Services, Inc. (SEL ES) group, where he is currently a Senior Engineer and supervisor. He performs event report analysis, relay settings and relay coordination, fault studies, and model power system testing using a real-time digital simulator. He is a registered professional engineer in the state of Washington and a member of IEEE.